Macromolecules
ARTICLE

*Macromolecules* **2010**, *43*, 6429–6437 **6429**
DOI: 10.1021/ma1008989

# Isomorphic Crystallization of Poly(hexamethylene adipate-*co*-butylene adipate): Regulating Crystal Modification of Polymorphic Polyester from Internal Crystalline Lattice

**Zhichao Liang, Pengju Pan, Bo Zhu, and Yoshio Inoue***

*Department of Biomolecular Engineering, Tokyo Institute of Technology, 4259-B-55 Nagatsuta, Midori-ku, Yokohama 226-8501, Japan*

*Received April 23, 2010; Revised Manuscript Received June 16, 2010*

ABSTRACT: The factors influencing the crystalline structure of polymorphic polymer have been investigated for random copolyester, poly(hexamethylene adipate-*co*-butylene adipate) (P(HA-*co*-BA)). P(HA-*co*-BA) exhibits isodimorphic crystallization. The crystalline modification of the PBA homopolymer type crystal was regulated via the isomorphic crystallization behavior of the HA and the BA units in P(HA-*co*-BA). The PBA $\beta$-form was preferred with increasing the HA unit content in the bulk copolymer due to the chain conformation of the HA homopolymer is selectively compatible with the crystalline lattice of the PBA $\beta$-form crystal. The temperature for complete or partial formation of the PBA $\alpha$-form crystal significantly increased with increasing the HA unit content. Particularly, the neat PBA $\beta$-form crystal was formed at 35 °C in P(HA-*co*-BA)(34/66). This study indicates that it is possible to achieve a precise regulation of crystalline modification of polymorphic polyester from the internal crystalline lattice via isomorphic crystallization.

## Introduction

Polymorphism is a widespread phenomenon in polymers.[1] Different crystalline forms of polymorphic polymers may arise from the different packing modes of the polymeric chains with different conformations, such as syndiotactic polypropylene (s-PP),[2] or different packing modes of molecular chains with identical conformation in the unit cell, as found for isotactic polypropylene (i-PP).[3−5] Generally, the physical properties of polymorphic polymers are dependent on their polymorphic modification. For instances, the $\beta$-form i-PP showed significantly improved toughness, drawability, and impact resistance compared to the $\alpha$-form i-PP;[6,7] the $\beta$-form of poly(vinylidene fluoride) (PVDF) shows the most highly polar phase among the various modifications ($\alpha$-, $\beta$-, $\delta$-, and $\gamma$-form).[8] Furthermore, the enzymatic and hydrolytic biodegradation kinetics of biodegradable polymers, such as poly(3-hydroxybutyrate) (P(3HB))[9,10] and poly(3-hydroxypropionate) (PHP),[11,12] are significantly influenced by the polymorphic crystalline structure.

Therefore, study on the effects of crystallization and processing conditions on the polymorphic behavior is essential to tailor the performance of these polymeric materials. Besides the crystallization temperature, crystallization methods, and stress, crystalline modification of polymorphic polymers can be regulated by many other factors. Molecular weight (MW) is a key factor affecting polymorphism of polymers, since polymers with different MWs usually have different thermodynamic parameters and crystallization kinetics.[13] The chain microstructure and the presence of comonomer units can also change the polymorphic behavior of polymers.[3,8,14,15] Because of the crystal memory effect, the starting structure, temperature, and time of fusion prior to crystallization might also influence the polymorphic behavior of polymers in the subsequent cold or melt-crystallization. Blending with miscible component usually alters the thermodynamic and kinetic environments and thus affects the crystalline structure of polymorphic polymers.[1,16] Moreover, the crystalline structure of polymorphic polymers can be controlled by epitaxial crystallization on the appropriate substrates[6] or utilization of appropriate nucleating agents due to the epitaxial mechanism.[6,17]

All of these factors influence the crystalline modification of polymorphic polyesters from the external of crystalline lattice. However, is it possible to control the polymorph from the internal of the crystalline lattice of polymorphic polymer? Herein, we would like to present a study of regulating the crystalline modification of polymorphic polyesters from the internal crystalline lattice via isomorphic crystallization.

The phenomenon of isomorphism has been detected for some random copolyesters, such as poly(propylene succinate-*co*-propylene terephthalate) [P(PSu-*co*-PT)][18] and poly(3-hydroxybutyrate-*co*-3-hydroxyvalerate) [P(3HB-*co*-3HV)].[19] Macromolecular isomorphism represents the statistical cocrystallization of different constitutional repeating units in a single isomorphic crystalline lattice.[1] Two requirements to macromolecular isomorphism were proposed by Allegra and Bassi:[20] (i) the different types of monomer units must have approximately the same shape and occupy the same volume, and (ii) the chain conformation of the parent homopolymers must be compatible with either crystal lattice. Comonomers in some copolymers of two or more alkylene dicarboxylate units cocrystallize into the same crystalline lattice, if the two comonomers have similar chemical structures and occupy approximately the same volume, such as poly(butylene succinate-*co*-ethylene succinate) [P(BS-*co*-ES)],[21] poly(butylene succinate-*co*-propylene succinate) [P(BS-*co*-PS)],[22] and poly(hexamethylene sebacate-*co*-hexamethylene adipate) [P(HSe-*co*-HA)].[23,24]

Poly(butylene adipate) (PBA) exhibits polymorphic crystallization behavior. It crystallizes in the $\alpha$- or $\beta$-form under different conditions. The $\alpha$-form is characterized by a monoclinic unit cell with dimensions of $a$ = 0.670 nm, $b$ = 0.800 nm, $c$ = 1.420 nm, and $\beta$ = 45.5°.[25] The $\beta$-form of PBA is characterized

*To whom correspondence should be addressed: Tel +81-45-924-5794; Fax +81-45-924-5827; e-mail inoue.y.af@m.titech.ac.jp.


Published on Web 07/15/2010

by chains in a planar zigzag conformation packed in an orthorhombic unit cell with lattice parameters of $a = 0.505$ nm, $b = 0.736$ nm, and $c$ (fiber axis) $= 1.467$ nm.[25,26] Poly(hexamethylene adipate) (PHA) was reported to form an orthorhombic unit cell with parameters $a = 1.008$ nm, $b = 1.464$ nm, and $c$ (fiber axis) $= 1.683$ nm.[28] Interestingly, the $d$-spacing values of the characteristic planes for the crystalline cell of PBA $\beta$-form crystal are very similar to those of PHA.[27,28] This may indicate the similarity of the structure between the PHA crystal and the PBA $\beta$-form crystal, despite their different crystalline unit cells. The HA and BA units seems to meet the requirements of cocrystallization in viewpoints of both the chemical structure and the crystalline structure. They are expected to be able to cocrystallize into the same crystalline lattice. Thus, the random poly(hexamethylene adipate-*co*-butylene adipate) [P(HA-*co*-BA)] copolyester is selected as a model for regulating the crystalline modification of polymorphic polyester from the internal crystalline lattice.

Some studies on the polymorphic control of PBA crystallization have been reported. Inoue and co-worker revealed that the novel PBA-inclusion complex with cyclodextrin acts as nucleating agent for enhanced formation of the PBA α-form crystal.[29,30] The PBA type polymorphic crystal can be formed within poly(butylenes adipate-*co*-butylene terephthalate) [P(BA-*co*-BT)] copolymers with the BT content less than 25 mol %, where the critical crystallization temperature for the formation of PBA α- and $\beta$-form crystal decreases with increasing the BT content due to restriction of the motion of the BA units by the BT unit in the molecular chain.[15] In these cases, the PBA α-form crystal was favored because it is more thermodynamically stable than the PBA $\beta$-form crystal. Can the formation of the PBA $\beta$-form crystal be regulated? As reported by Gan and co-worker,[31,32] the PBA crystal modification can be controlled by the epitaxial crystallization on the substrate polymers, such as highly oriented PE and i-PP, due to the excellent matching of lattice between the PBA modification and the crystal of the substrates. However, all of these modifications for polymorphs of PBA crystal originate from the environmental inducing or restriction of the crystalline lattice in the crystallization process. Moreover, despite the extensive research has been conducted on the crystallization behavior and solid-state structure of random copolyesters, it remains to be clarified how the comonomer units influence the packing state of the host units in the cocrystal.

In this study, the crystallization behavior and crystalline structure of P(HA-*co*-BA) copolyester will be analyzed in order to study the regulation of the polymorphs of PBA from the internal lattice cell and how the crystalline structure of the host units is affected by the comonomer units.

## Experimental Section

**Materials.** PBA was purchased from the Sigma-Aldrich Co. Ltd. (St. Louis, MO) and used directly. PHA and the copolymer P(HA-*co*-BA) were synthesized from hexanediol (HD), butanediol (BD), and adipic acid with various feeding molar ratios of BD/HD by thermal polycondensation at 160 °C in a nitrogen atmosphere for 2 h and then in a vacuum at 200 °C for 8−12 h. Stannous chloride was used as the catalyst. The products were purified by the dissolving−precipitating method with chloroform (solvent)/ethanol (nonsolvent) and then dried at 60 °C under vacuum for 24 h. The number- and weight-average molecular weights ($M_n$, $M_w$) and their distributions (polydispersity index: PDI) of polyester samples were determined by gel permeation chromatography (GPC) system (Tosoh Co., Tokyo, Japan). The comonomer compositions of the copolymers were determined using $^1$H NMR and $^{13}$C NMR. Both the 600 MHz $^1$H NMR and 150 MHz $^{13}$C NMR spectra were recorded on a Bruker AVANCE 600 spectrometer (Bruker BioSpin K.K, Osaka, Japan) using deuteriochloroform ($CDCl_3$) as the solvent. The chemical shifts reported were referenced to internal tetramethylsilane (0.00 ppm) or the solvent resonance at the appropriate frequency.

**DSC.** The nonisothermal crystallization behavior of the polymer samples were investigated by a Pyris Diamond differential scanning calorimeter (DSC) (Perkin-Elmer Japan Corp., Yokohama, Japan) under a nitrogen atmosphere. The scales of temperature and heat flow at different heating rates were calibrated using an indium standard. The samples were weighted and sealed in an aluminum pan. In the nonisothermal melt-crystallization, the samples were melted at 100 °C for 2 min before being cooled to 50 °C under a cooling rate of 10 °C/min. An intracooler was connected to the DSC apparatus to achieve reliability at high cooling rates over the whole temperature range of the experiments.

**FTIR Spectroscopy.** The copolymer samples were observed on an Fourier transform infrared (FTIR) spectrometer (Shimadzu Co. Ltd., Kyoto, Japan) equipped with an AIM-8800 multichannel infrared microscope (Shimadzu Co. Ltd., Tokyo, Japan) and a MCT detector in the transmission mode. P(HA-*co*-BA) sample was placed between two pieces of $BaF_2$ slides, and then it was melted at 100 °C for 2 min before quenched to the desired $T_c$. For studying the crystalline structure, the FTIR spectra of all crystallized samples were measured at 25 °C to erase the temperature effect on the IR spectra. After the melt-crystallization, the sample was heated from $T_c$ to 100 at 1 °C/min in a LK-600FTIR hot stage (Japan High Tech Co., Ltd., Fukuoka, Japan) for studying the melting behavior. The FTIR spectra were recorded at a 1 °C interval during the heating process, and the spectra were collected with 32 scans and a resolution of 2 $cm^{-1}$.

**X-ray Analysis.** The crystalline structure of polymer sample was investigated by wide-angle X-ray diffraction (WAXD) analysis with a Rigaku RU-200 (Rigaku Corp., Tokyo, Japan), working at 40 kV and 200 mA, with Ni-filtered Cu Kα radiation ($\lambda = 0.154\,18$ nm). WAXD patterns were recorded in the $2\theta$ range of 5°−50° at a scanning rate of 2°/min. Assuming that the diffraction peaks from a crystallographic plane and the amorphous halo could be reproduced by a Gaussian curve and a sum of two Gaussian curves, respectively, diffraction patterns in the $2\theta$ range of 5°−50° were resolved into a series of Gaussian peaks by curve-fitting using the damped least-squares algorithm. The degree of crystallinity was calculated from the relative areas of the resolved peaks. The samples for the WAXD analysis were prepared by a hot press at 100 °C and then crystallized at the desired temperatures.

## Results and Discussion

**Characterization of Copolymers.** First, the comonomer composition in P(HA-*co*-BA) copolymers was estimated from $^1$H NMR spectra using the relative intensities of proton peaks arising from hexamethylene adipate (HA) and butylene adipate (BA) repeating units. Figure 1 shows the $^1$H NMR spectra of PHA, PBA, and P(HA-*co*-BA)(50/50). The $^1$H NMR spectra of PHA and PBA show characteristic peaks at 4.08 and 4.12 ppm, which may be assigned to the α methylene proton of hexanediol and *f* methylene protone of butanediol, respectively. The content of the HA units in P(HA-*co*-BA)(45/55) was estimated to be 45 mol %, using the relative intensities of the peaks at 4.08 and 4.12 ppm. Here, the samples are referenced using the molar ratio of HA/BA in copolymers. In this study, copolymers of P(HA-*co*-BA)(16/84), P(HA-*co*-BA)(26/74), P(HA-*co*-BA)-(34/66), P(HA-*co*-BA) (45/55), P(HA-*co*-BA)(62/38), P-(HA-*co*-BA)(76/24), and PHA were synthesized. The error range of comonomer unit composition was estimated to be ±2%.

The results for characterization of all copolymer samples are summarized in Table 1. The comonomer unit composition in the copolymer shows only a small deviation from the feeding molar ratio of hexanediol and butanediol, indicating that the comonomer unit composition in P(HA-*co*-BA) copolymers can be easily controlled by adjusting the feeding molar ratio of two diols. The number-average molecular weight and the PDI of copolymers, as estimated by GPC, were in the range $(1.1-1.6) \times 10^4$ and 1.3−1.5, respectively.

The comonomer sequence distribution of P(HA-*co*-BA) copolymers was determined using $^{13}$C NMR spectroscopy. In Figure 2a are shown the assignments of $^{13}$C resonances absorptions of different carbons in the polymer chain of P(HA-*co*-BA)(45/55). Particularly, the $^{13}$C resonances at 33.87 and 33.80 ppm are assigned to the methylene carbon

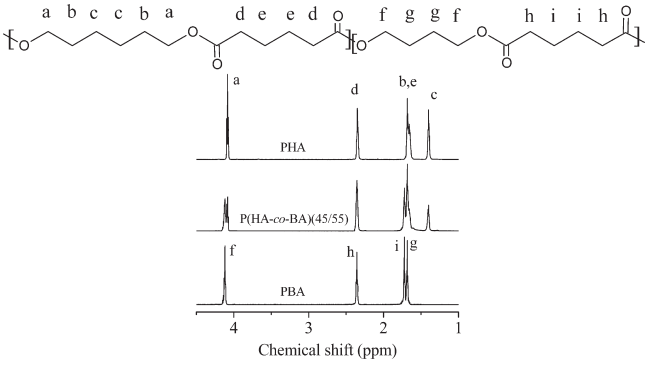


**Figure 1.** $^1$H NMR spectra of PHA, PBA, and P(HA-*co*-BA)(45/55) copolymer.

ε in PHA and ε′ in PBA, respectively, as shown in Figure 2b, and the ratios of integrated intensity of resonance absorption of ε:ε′ are equal to the molar ratios of the HA:BA units in each P(HA-*co*-BA) samples. Moreover, in the $^{13}$C NMR spectra of copolymer samples, the resonance of carbons ε and ε′ were found to be the superposition of the resonances at 33.87, 33.84 ppm and those at 33.82, 33.80 ppm, which may respectively correspond to the carbon ε in the hexamethylene−adipate−hexamethylene (HAH), the methylene carbon ε closest to the hexamethylene unit in the hexamethylene−adipate−butylene (HAB) units, the methylene carbon ε′ closest to the butylene unit in the hexamethylene−adipate−butylene (HAB), and the butylene−adipate−butylene (BAB) units. By integrating corresponding resonances, the content of HAH, HAB/BAH, and BAB triads were estimated for all the P(HA-*co*-BA) copolymers, as summarized in Table 2. Meanwhile, the relative distributions of HAH, HAB/BAH, and BAB triads in statistically random P(HA-*co*-BA) copolymers are also calculated and summarized in Table 2. The experimental and the theoretically calculated values for P(HA-*co*-BA) copolymers are in good agreement with each other, indicating that all of the prepared P(HA-*co*-BA) samples are nearly random copolymers.

**Isodimorphic Crystallization of P(HA-*co*-BA).** The nonisothermal crystallization and the subsequent melting process of P(HA-*co*-BA)s were investigated by DSC, as shown in Figure 3. For all samples, one single crystallization peak was observed. In the melting process, single melting peaks were observed for all samples except PBA. As summarized in Table 1, high values of melting enthalpy were observed for all samples. These results may indicate the occurrence of the cocrystallization of the two comonomer units in the same

**Table 1. Feed Monomer Molar Ratios in Copolymerization Reaction Reactor and Comonomer Composition, Molecular Weight Parameters, Melting Temperatures, Heat of Fusion, and Degree of Crystallinity of P(HA-*co*-BA)s**

| sample code (molar ratio of HA/BA) | HA/BA molar ratio in feed | HA/BA molar ratio in copolymer[a] | $M_n$[b] | $M_w$[b] | PDI[b] | $T_m$[c] (°C) | $\Delta H_m$[c] (J/g) | crystallinity[d] (%) |
|---|---|---|---|---|---|---|---|---|
| 0/100 | 0/100 | 0/100 | $0.9 \times 10^4$ | $1.2 \times 10^4$ | 1.33 | 51.2 | 76 | 79.7 |
| 16/84 | 15/85 | 16/84 | $1.2 \times 10^4$ | $1.6 \times 10^4$ | 1.33 | 46.0 | 79 | 73.1 |
| 26/74 | 25/75 | 26/74 | $1.0 \times 10^4$ | $1.5 \times 10^4$ | 1.50 | 37.4 | 83 | 66.7 |
| 34/66 | 40/60 | 34/66 | $1.6 \times 10^4$ | $2.1 \times 10^4$ | 1.31 | 37.0 | 82 | 64.3 |
| 45/55 | 50/50 | 45/55 | $1.2 \times 10^4$ | $1.7 \times 10^4$ | 1.42 | 32.1 | 85 | 62.1 |
| 62/38 | 60/40 | 62/38 | $1.2 \times 10^4$ | $1.8 \times 10^4$ | 1.50 | 39.0 | 87 | 71.5 |
| 76/24 | 75/25 | 76/24 | $1.1 \times 10^4$ | $1.5 \times 10^4$ | 1.36 | 46.7 | 88 | 71.0 |
| 100/0 | 100/0 | 100/0 | $1.6 \times 10^4$ | $2.4 \times 10^4$ | 1.50 | 59.8 | 92 | 71.7 |

[a] Comonomer unit composition of P(HA-*co*-BA) was estimated by $^1$H NMR analysis, $\delta = \pm 2\%$; the fraction numbers indicate the molar ratio of HA/BA in the whole copolymer. [b] $M_n$, $M_w$, and PDI were measured by GPC analysis. [c] $T_m$ and $\Delta H_m$ were obtained by DSC at a heating rate of 10 °C/min after a melt-crystallization process. [d] The crystallinity for samples crystallized at 25 °C was measured by WAXD, with $\delta = \pm 5\%$.

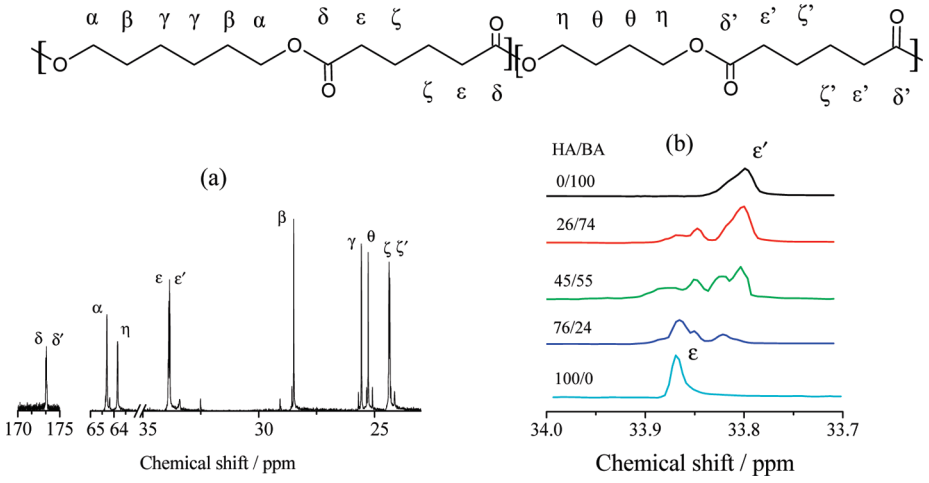


**Figure 2.** $^{13}$C NMR spectrum of (a) P(HA-*co*-BA)(45/55) and (b) P(HA-*co*-BA) (0/100, 26/74, 45/55, 76/24, and 100/0) at the 34.0−33.7 ppm region.

**Table 2. Distribution of Selected Triads for P(HA-*co*-BA) Copolymers**

| HA/BA molar ratio in polymer | HAH (%) | | HAB + BAH (%) | | BAB (%) | |
|---|---|---|---|---|---|---|
| | obsd[a] | calcd[b] | obsd[a] | calcd[b] | obsd[a] | calcd[b] |
| 16/84 | 2.1 | 2.6 | 25.0 | 26.9 | 72.9 | 70.5 |
| 26/74 | 5.7 | 6.8 | 35.4 | 38.5 | 58.9 | 54.7 |
| 34/66 | 13.1 | 11.5 | 47.6 | 44.9 | 39.3 | 43.6 |
| 45/55 | 22.7 | 20.3 | 49.0 | 49.5 | 28.3 | 30.2 |
| 62/38 | 36.6 | 38.4 | 48.5 | 47.1 | 14.9 | 14.5 |
| 76/24 | 62.2 | 57.8 | 32.8 | 36.5 | 5.0 | 5.7 |

[a] Measured from the $^{13}C$ NMR by curve-fitting. [b] Calculated for a random P(HA-*co*-BA) copolymer.

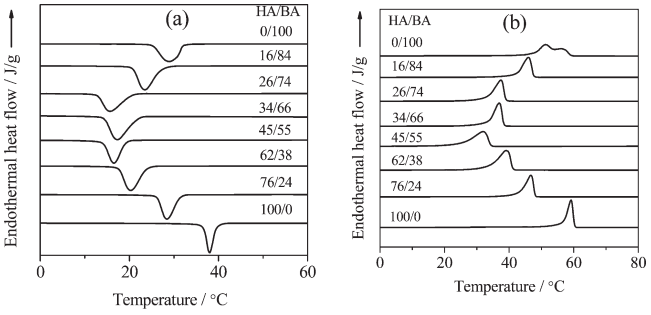


**Figure 3.** (a) DSC nonisothermal crystallization curves at a cooling rate of 10 °C/min and (b) subsequent melting curve at a heating rate of 10 °C/min.

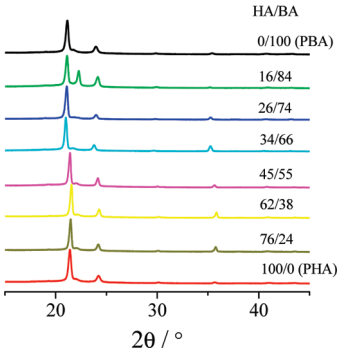


**Figure 4.** WAXD patterns of P(HA-*co*-BA) samples crystallized at 25 °C.

crystalline lattice cell. Note that the melting enthalpy generally increased with increasing the HA unit content. This may be attributed to that the content of HA unit in the crystalline lattice increased with increasing the HA unit content in the bulk. Moreover, a depression of both crystallization and melting temperatures with increasing the comonomer unit content was observed for P(HA-*co*-BA)s. As a result, the lowest crystallization and melting temperatures were observed for P(HA-*co*-BA)(45/55). As reported by the studies on the cocrystallization behavior of aliphatic copolyesters,[20−24] such a behavior may indicate the occurrence of isodimorphism in these copolyesters. Further analysis of the crystalline structure was performed with WAXD.

The WAXD patterns of P(HA-*co*-BA)s crystallized at 25 °C are shown in Figure 4. The degree of crystallinity was calculated from the WAXD and also summarized in Table 1. The degree of crystallinity is higher than 62% for all copolymers. This is consistent with the high melting enthalpy observed by DSC measurement. Moreover, the crystallinity of copolyester samples crystallized at 25 °C generally decreased with increasing comonomer units. This may be attributed to the effect of undercooling on the cocrystallization of comonomer units. The PBA crystallized at 25 °C

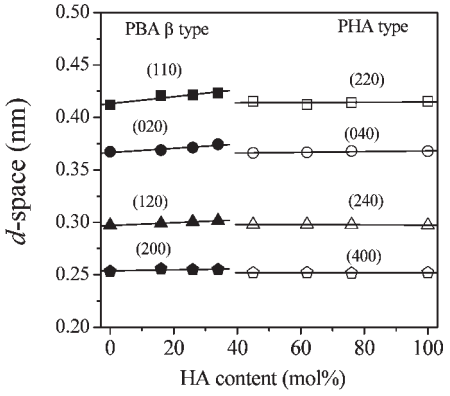


**Figure 5.** *d*-spacing of characteristic planes for P(HA-*co*-BA)s crystallized at 25 °C.

forms the $\beta$-form crystal.[33,34] Its WAXD pattern was similar to that of PHA, but the peak of its (110) plane appears at lower $2\theta$ angle than that of the PHA (220) plane. For all of the copolyesters, two kinds of crystalline structure were observed. As shown in Figure 4, for copolymers with the HA unit content up to 34 mol %, the PBA type crystalline structure develops, i.e., the PBA lattice accommodates the HA units; meanwhile, for copolymers with the HA unit content higher than 45 mol %, the PHA type crystalline structure develops. In accordance with the DSC results, these WAXD patterns confirmed the isodimorphic crystallization of P(HA-*co*-BA)s.

The *d*-spacing values of the crystalline planes of P(HA-*co*-BA)s were calculated with the Bragg equation. In Figure 5, the plots of *d*-spacing versus the HA unit content (mol %) were presented for the (110), (020), (120), and (200) planes of the PBA $\beta$-form crystal (orthorhombic unit cell, $a$ = 0.505 nm, $b$ = 0.736 nm, $c$ = 1.467 nm) as well as the (220), (040), (240), and (400) planes of PHA type crystal (orthorhombic unit cell, $a$ = 1.008 nm, $b$ = 1.464 nm, $c$ = 1.683 nm).[25−28] As shown in Figure 5, the *d*-spacing of the (110), (020), (120), and (200) planes of the PBA $\beta$-form crystal increased with increasing the HA unit content in copolymer, indicating that the inclusion of the HA units into the crystalline lattice of the PBA $\beta$ type crystal results in the slight expansion of the unit size and the content of the HA units included in the host crystalline lattice increased with increasing the HA unit content in the bulk polymer. On the other hand, the increase of the BA units in the copolymer from 0 to 38 mol % did not show significant influence on the crystalline structure of the PHA type crystal although a small enlargement in the unit size of crystalline lattice was observed at the BA unit content of 55 mol %. This suggests that the BA segments are highly compatible with the HA segments in the PHA type crystal. Hence, the PHA type crystal does not have to enlarge its unit cell in order to include the BA unit.

It is well-known that the comonomer concentration in the crystalline lattice of copolymer is strongly dependent on the comonomer composition and crystallization conditions. Be worthy of noting, both the WAXD pattern of (020) in the PBA α-form crystal and that of (110) in the PBA β-form crystal were found in P(HA-*co*-BA)(16/84), indicating the coexistence of both PBA α- and β-form crystals in P(HA-*co*-BA)(16/84). However, only the PBA β-form crystals were developed in the copolymers with 26 and 34 mol % HA units. These results clearly demonstrated that the formation of the PBA type crystal was affected by the HA unit content. The PBA β-form crystals were preferred with increasing the HA unit content in the copolymers.

As IR spectrum is sensitive to the conformation and the packing state of polymer chains, it was applied to investigate the crystalline phase of P(HA-*co*-BA) copolymers. Figure 6 shows the IR spectral changes of P(HA-*co*-BA) in the region of 1100−850 $cm^{-1}$ as the HA unit content in the copolymers increases from 0 to 100 mol %.

The crystalline bands of PBA appeared at 910 and 930 $cm^{-1}$ were assigned as the characteristic crystalline bands of the PBA β-form crystal, and that at 909 $cm^{-1}$ was assigned to the PBA α-form crystal, while those at 911 and 921 $cm^{-1}$ were assigned as the crystalline bands of the PHA type crystal. It is interesting to find that the crystalline band at 930 $cm^{-1}$ appears in the IR spectra of P(HA-*co*-BA) copolymers with the PBA type crystal, indicating the existence of PBA β-form crystal. This result is in good agreement with that of WAXD. The intensity of the band at 930 $cm^{-1}$ decreased with increasing HA content in the copolymer. Meanwhile, the intensity of the band at 921 $cm^{-1}$ increased with increasing the HA unit content. The IR bands appeared at 971 and 1080 $cm^{-1}$ are assigned as the characteristic crystalline bands for PHA and those at 960 and 1066 $cm^{-1}$ for PBA, respectively. In the in-situ FTIR measurements of P(HA-*co*-BA) copolyesters in the melt-crystallization and the subsequent melting process of samples, all the intensities of these characteristic bands at 1080, 1066, 971, and 960 $cm^{-1}$ synchronously increase with time in the crystallization process, decrease in the heating process, and finally disappear in the melt. These results indicate the coexistence of the HA and BA units in the crystalline phase of copolymers. Therefore, it provides a further evidence for the occurrence of cocrystallization of the HA and the BA units in the crystalline lattice of P(HA-*co*-BA).

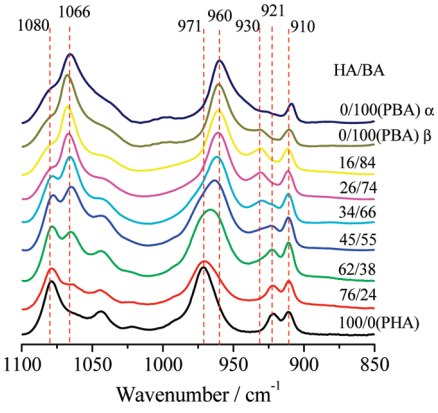


**Figure 6.** IR spectra of P(HA-*co*-BA)s crystallized at 25 °C.

**Effect of the HA Unit on the Polymorphic Crystallization of the PBA Type Crystal.** PBA shows temperature-dependent polymorphic crystallization behavior.[33,34] In order to comprehensively understand the crystallization behaviors of the PBA type crystal in P(HA-*co*-BA)s, the isothermal crystallization of P(HA-*co*-BA)s forming the PBA type crystal was investigated with FTIR and WAXD.

Parts a and b of Figure 7 show the IR spectra in the region of 1050−800 $cm^{-1}$ for P(HA-*co*-BA)(16/84) isothermally crystallized at $T_c$ = 30−36 °C and P(HA-*co*-BA) (26/74) at $T_c$ = 25−35 °C, respectively. In P(HA-*co*-BA)(16/84) and (26/74), the crystalline band at 930 $cm^{-1}$ significantly decreased at crystallization temperatures higher than 32 °C, and it disappeared at 36 °C in P(HA-*co*-BA)(16/84). Meanwhile, the band at 910 $cm^{-1}$ shifted to 909 $cm^{-1}$ as $T_c$ increased to a temperature higher than 32 °C. Since the crystalline bands at 930 and 910 $cm^{-1}$ are assigned as the characteristic bands for PBA β-form crystal and that at 909 $cm^{-1}$ for PBA α-form crystal, this result indicates the crystalline phase transition of PBA type crystal from the β-form to the α-form with increasing the crystallization temperature. However, the crystalline bands at 930 and 910 $cm^{-1}$ in P(HA-*co*-BA)(34/66), as shown in Figure 7c, was almost not varied with $T_c$, indicating that a stable PBA type crystal

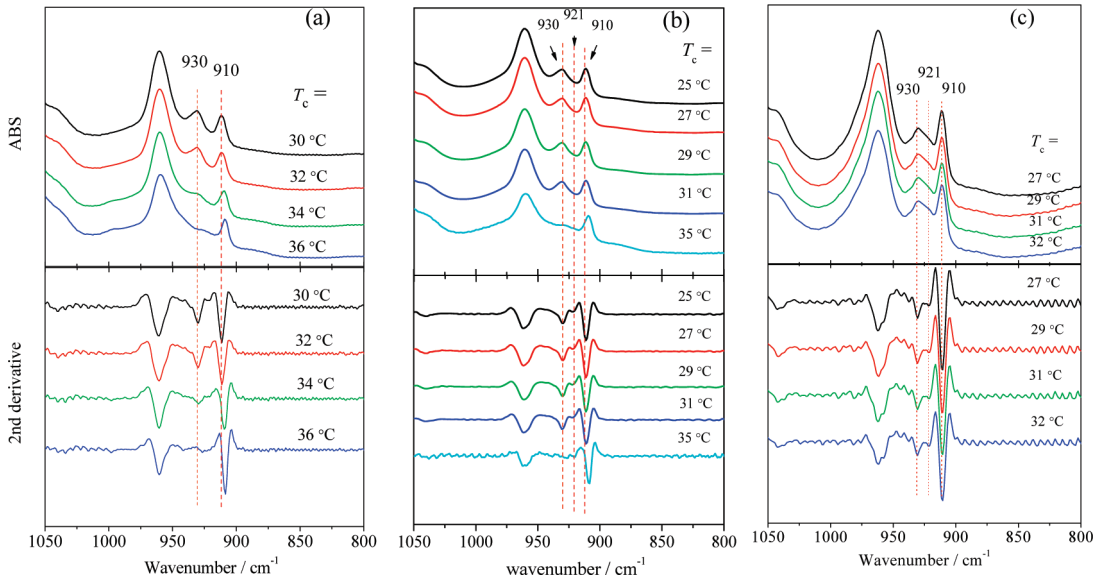


**Figure 7.** IR spectra in the 1050−800 $cm^{-1}$ region and the second derivative of the IR spectra of (a) P(HA-*co*-BA)(16/84) crystallized at 30−36 °C, (b) P(HA-*co*-BA)(26/74) crystallized at 25−35 °C, and (c) P(HA-*co*-BA)(34/66) crystallized at 27−32 °C.

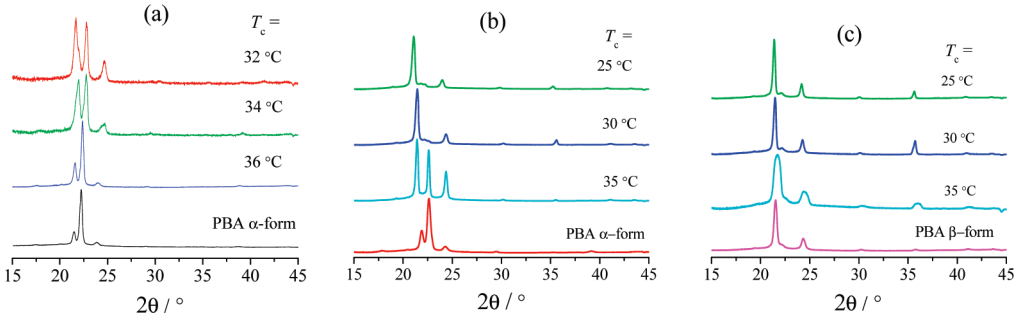


**Figure 8.** WAXD patterns of (a) P(HA-*co*-BA)(16/84) crystallized at 30−36 °C, (b) P(HA-*co*-BA)(26/74) crystallized at 25−35 °C, and (c) P(HA-*co*-BA)(34/66) crystallized at 25−35 °C.

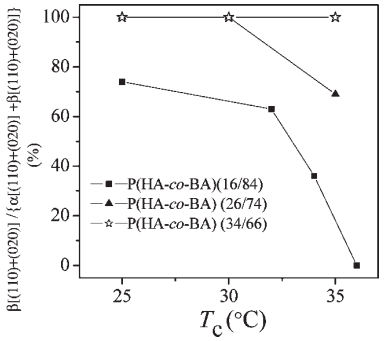


**Figure 9.** Relative integrated intensity of the PBA $\beta$[(110) + (020)] plane, $\beta$[(110) + (020)]/{α[(110) + (020)] + $\beta$[(110) + (020)], formed in the isothermal crystallization.

was formed in P(HA-*co*-BA)(34/66) despite the increased crystallization temperatures. Moreover, it is worthy of noting that the crystalline band at 921 $cm^{-1}$ can be observed in all of these samples, indicating the inclusion of the HA units in the crystalline lattice of the PBA type crystal. Therefore, the polymorphic phase behavior was observed in the isomorphic crystal of P(HA-*co*-BA). Furthermore, the polymorphic crystallization behavior of the PBA type crystal in P(HA-*co*-BA) was influenced not only by the crystallization temperature but also by the HA unit content.

In Figure 8 are shown the WAXD patterns of P(HA-*co*-BA)(16/84) isothermally crystallized at $T_c$ = 32−36 °C, P(HA-*co*-BA)(26/74) at $T_c$ = 25−35 °C, and P(HA-*co*-BA)-(34/66) at $T_c$ = 25−35 °C. The relative area of the PBA $\beta$[(110) + (020)] and α[(110) + (020)] planes formed in the isothermal crystallization were roughly evaluated by calculating the relative integrated intensities of the crystalline bands of PBA α[(110) + (020)] and $\beta$[(110) + (020)] planes in the WAXD patterns, as presented in Figure 9.

As shown in Figure 8a, the WAXD patterns of P(HA-*co*-BA)(16/84) crystallized at 32 and 34 °C were similar to those crystallized at 25 °C, indicating that both of the PBA α- and $\beta$-form crystal were formed during the isothermal crystallization process at 32 and 34 °C. Moreover, as the crystallization temperature increased from 25 to 36 °C, the transition from the PBA $\beta$- to α-form crystal was observed. As shown in Figure 9, the relative integrated intensities of the PBA $\beta$[(110) + (020)] planes, $\beta$[(110) + (020)]/{α[(110) + (020)] + $\beta$[(110) + (020)]}, significantly decreased as the crystallization temperature increased from 25 to 34 °C. When the crystallization temperature increased up to 36 °C, the crystalline modification of P(HA-*co*-BA)(16/84) was totally converted to the PBA α-form crystal. These demonstrate that the polymorphic crystallization behavior occurs in the isothermal crystallization of P(HA-*co*-BA)(16/84). Furthermore, the WAXD patterns of P(HA-*co*-BA)(26/74) is particularly of interest, as shown in Figure 8b. As the crystallization temperature increased from 30 to 35 °C, the crystalline structure of copolymer transferred from neat PBA $\beta$-form crystal to the coexistence of both the PBA α- and $\beta$-form crystal; i.e., the value of $\beta$[(110) + (020)]/{α[(110) + (020)] + $\beta$[(110) + (020)]} decreased from 100/100 to about 70/100, as shown in Figure 9. On the other hand, further increase of the HA units in the copolymer makes lost the temperature effect on the phase transition of PBA type crystal formed in P(HA-*co*-BA). As shown in Figure 8c, the crystalline structure of P(HA-*co*-BA)(36/64) was almost unchanged despite of the increase of $T_c$ from 25 to 35 °C, indicating that the PBA $\beta$-form crystal was surprisingly formed even at 35 °C.

As reported by Gan et al.,[15,33] the PBA α-form crystal, the $\beta$-form crystal, and the mixture of α- and $\beta$-crystal forms grow at the crystallization temperatures above 32 °C, below 27 °C, and between these two temperatures, respectively. Comparing the temperature-dependent phase transition behavior in PBA and in the PBA type crystal of P(HA-*co*-BA), some interesting results were found. First, in P(HA-*co*-BA)-(16/84) the PBA α-form crystal grew at 36 °C, and the coexistence of the PBA α- and $\beta$-form crystal was observed for samples crystallized at the temperature ranged from 25 to 34 °C. Second, in P(HA-*co*-BA)(26/74) the PBA $\beta$-form crystal grew at 30 °C, and the mixture of the PBA α- and $\beta$-form crystal was observed for the sample crystallized at 35 °C. These results significantly demonstrate the effect of the HA unit content on the polymorphic crystallization behavior of the PBA type crystal.

In P(HA-*co*-BA)(16/84), the BA unit is the dominant factor in determining the crystalline structure. The PBA $\beta$-form crystal tends to include the HA units into its crystalline lattice, since the energy penalty for inclusion of the HA unit is very low. This may result in the decrease of the crystallization temperature of the PBA $\beta$-form crystal. On the other hand, the PBA α-form crystal may tend to exclude the HA units from the crystalline phase due to the difference in packing state between the HA and the BA unit in the PBA α-form crystal. The polymorphic transition from the PBA $\beta$- to α-form crystal as the crystallization temperature increased from 25 to 36 °C should be ascribed to two reasons. First, the formation of more perfect crystal may be required at a higher crystallization temperature. Hence, more HA units are excluded from the PBA crystalline lattice with increasing $T_c$. Secondary, the PBA α-form crystal is more thermodynamically stable than the $\beta$-form. Hence, if the HA unit is not included in the crystalline lattice, the PBA α-form crystal should be highly preferred at crystallization temperatures higher than 32 °C. As a result, a transition from the PBA α + $\beta$ form to the neat α-form crystal as the crystallization

**Table 3. Value of *d*-Spacing of the Characteristic Planes of PHA and PBA α- and *β*-Type Crystal**

| PHA[a] | | PBA (*β* type)[b] | | PBA (α type)[b] | |
|---|---|---|---|---|---|
| index | $d_{measd}$ (nm) | index | $d_{measd}$ (nm) | index | $d_{measd}$ (nm) |
| 220 | 0.415 vs | 110 | 0.416 vs | 110 | 4.11 |
| 040 | 0.366 vs | 020 | 0.367 vs | 020 | 3.97 |
| 240 | 0.296 w | 120 | 0.297 w | 120 | 3.06 |
| 400 | 0.252 s | 200 | 0.253 m | 200 | 2.40 |

[a] From ref 28. [b] From ref 27.

temperature increased to 36 °C was observed in P(HA-*co*-BA)(16/84). This result indicates that the polymorphic transition of the PBA crystal in P(HA-*co*-BA)(16/84) is influenced by the cocrystallization of the HA and the BA units in the same crystalline lattice.

The cases of P(HA-*co*-BA)(26/74) and P(HA-*co*-BA)(34/66) should be different from that of P(HA-*co*-BA)(16/84) because the HA unit content in the former samples is higher than the latter. Since the relatively long BA sequences necessitated for forming stable PBA crystal decreased with increasing the HA unit content, the entropy gain upon the cocrystallization becomes large, and it shall increase with the HA unit content. Therefore, the tendency for the cocrystallization of the HA and the BA units in the crystalline lattice is preferred thermodynamically. The preference of inclusion of large amount of the HA units makes the advantage of adopting the PBA *β*-form over the α-form crystal in P(HA-*co*-BA)(26/74) and P(HA-*co*-BA)(34/66). However, when the crystallization temperature is as high as 35 °C, the high crystallization temperature enables some relatively long BA sequence to exclude the HA units from the crystalline lattice so as to form more perfect PBA crystal in P(HA-*co*-BA)(26/74). On the other hand, further increase of the HA unit content decreases the length of the BA sequence and prevents the formation of stable neat PBA crystal where all the HA units are excluded. Therefore, the PBA *β*-form was formed in P(HA-*co*-BA)(34/66) even at 35 °C. These results further manifest that the cocrystallization of the HA and the BA units in the crystalline lattice is the crucial factor influencing the polymorphic transition of the PBA crystal in P(HA-*co*-BA) copolyester.

Above all, the polymorphic crystallization behavior of the PBA type crystal in P(HA-*co*-BA)s sufficiently demonstrated that the polymorphic modification of PBA can be controlled by the cocrystallization of the HA and BA units in the crystalline lattice of P(HA-*co*-BA). The cocrystallization of the HA and BA units in the PBA type crystal is generally achieved as the inclusion of the HA units into the PBA *β*-form crystal. Moreover, the included HA units in the PBA crystal functioned as the stabilizer for the PBA *β*-form crystal even at a high crystallization temperature of 35 °C. Therefore, it is reasonable to state that the polymorphic modification of PBA can be regulated from the internal crystalline lattice.

As an example for regulating the polymorphic modification from the internal crystalline lattice, the regulation of the crystalline modification of the PBA crystal in P(HA-*co*-BA)s is on account of two reasons. First, as shown in Table 3, the *d*-spacing values for the planes (220), (040), (240), and (400) of PHA[28] were rather close to those of the planes (110), (020), (120), and (200) in the PBA *β*-form crystal,[27] but different from those of the planes (110), (020), (120), and (200) in the PBA α-form crystal, indicating that the chain conformation and the packing form in the PHA crystal are similar to those in the PBA *β*-form crystal but different from those in the PBA α-form crystal. As a result, the energy penalty for

**Scheme 1. Regulation of the Crystalline Modification of PBA via Isomorphic Crystallization**

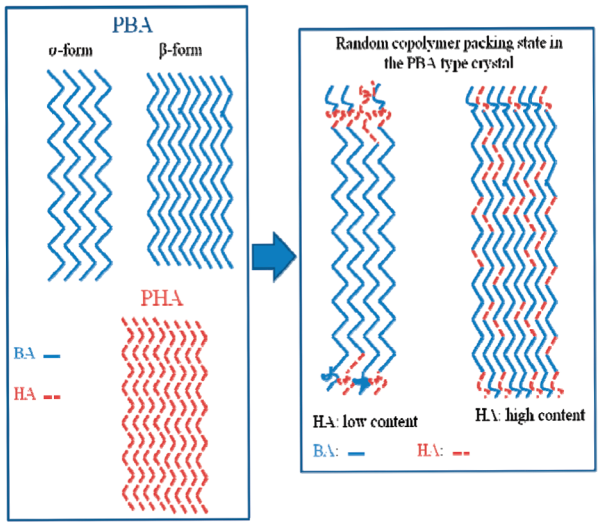


including the HA units in the PBA *β*-form crystalline lattice is much lower than that in the PBA α-form. Therefore, the cocrystallization of the HA and BA units into the PBA *β*-form crystal is thermodynamically favored, particularly for the copolymer with higher HA unit content. In other words, the isomorphic crystallization of P(HA-*co*-BA) forming the PBA type crystal was oriented by the HA unit.

Second, the included HA units in the PBA *β*-form crystal prevent the transition of the PBA type crystal from *β*- to α-form even at a high crystallization temperature. Despite the PBA α-form crystal is more thermodynamically stable than the *β*-form crystal, the transition of the PBA *β*- to α-form in the cocrystal of P(HA-*co*-BA) has to exclude all of the HA units from the crystalline lattice. However, with increasing the HA unit content in the molecular chain, the formation of neat PBA crystal becomes rather difficult that the transition of the PBA *β*- to α-form is inhibited even at high crystallization temperature. As a result, the stable PBA *β*-form crystal was formed even at 35 °C. These results indicate that it is possible to apply the selective isomorphic crystallization of random copolyester for regulating the crystalline modification of polymorphic polyester.

The mechanism of regulating the crystalline modification of PBA type crystal formed in P(HA-*co*-BA) can be elucidated in Scheme 1. In P(HA-*co*-BA), an isodimorphic crystallization behavior has been detected. In the PBA type crystal, the chain conformation of the included HA units is selectively compatible with the crystalline lattice of PBA *β*-form crystal. Therefore, the modification of PBA *β*-form crystal is highly favored in the melt-crystallization process, indicating the crystalline modification of PBA can be easily controlled in process. Moreover, the modification of the PBA can be further controlled by adjusting the content of the HA unit in bulk copolymer. At low content of the HA unit, some or most of the HA units may be excluded from the crystalline lattice of the PBA type crystal. Then, a coexistence of the PBA α- and *β*-form crystal or neat PBA α-form crystal may be obtained in the melt-crystallization process. At high content of HA unit, the PBA *β*-form should be highly preferred thermodynamically, since it is impossible to exclude all the HA units from the crystalline lattice of PBA.

Despite many isomorphic random copolymer systems with polymorphic comonomeric unit have been investigated and the influence of the comonomeric unit on the polymorphic crystallization has been elucidated for some systems, the

precise regulation of the crystalline modification of the polymorphic polymer from the internal crystalline lattice was rarely revealed. For example, the BT unit in the PBA type crystal of P(BA-*co*-BT) was reported to influence the polymorphic crystallization of PBA type crystal due to restrictive effect of the BT units on the BA segments in the polymer chain.[15] Though the cocrystallization of the BA and BT units in the crystalline phase was proved by solid-state NMR analysis,[35] the BT units did not show any selectivity on the PBA α- or $\beta$-form crystal. Therefore, such an influence is an environmental impact rather than a precise control arisen from the internal crystalline lattice.

As reported by De Rosa et al., the crystalline modification of the polymorphic isotactic polypropylene (iPP) and syndiotactic polypropylene (sPP) can also be regulated by the incorporated comonomeric units.[36−41] The comonomer units play a double role in the polymorphic iPP.[36,37] The first effect that favors crystallization of the $\gamma$-form is the interruption of the regular isotactic propylene sequences with shortening of the average length of the crystallizable sequences. The second effect is due to the possible inclusion of defects in the crystals of the polymorphic forms of iPP that favors the crystallization of α- and $\gamma$-forms depending on which of the two forms better tolerates the defect within its crystalline lattice. The syndiotactic propene−butene copolymers crystallize in the whole range of comonomer composition in disordered modifications intermediate between the *B*-centered form I of sPP and the *C*-centered form I of syndiotactic poly(1-butene) (sPB) (or *C*-centered the form II of sPP), which are indeed the crystal forms characterized by chains in 2-fold helical conformation packed in orthorhombic unit cells according to similar modes of packing.[38−41] Upon stretch, the phase transition from the helical form I of sPP into the trans-planar form III was prevented by the increasing butane content in the sPPBu copolymers because the butene units are rejected from crystals of form III but easily included in crystals of the helical forms of sPP.[41]

The cases of iPP are slightly different from the PBA in this study. The constitutional defects in iPP play a double role rather than the selective compatibility with different crystal forms of iPP. This may be because that the stereo/regio structure of iPP is much more complicated than the simply linear copolyester as discussed in this study. However, the case of the syndiotactic propene−butene copolymers is close to the P(HA-*co*-BA) copolymers in this study. First, because of the similar crystal structures of sPP and sPB, the syndiotactic propene−butene copolymers crystallize in the whole range of comonomer compositions, adapting either the sPP type crystal or the sPB type crystal. Thus, they may be considered as the so-called isomorphic copolymer. Moreover, the incorporated butene units in sPP crystal exhibit selectivity among the crystal of helical forms and the crystal of transplanar form of sPP. Therefore, the isodimorphic P(HA-*co*-BA)s copolyester and the syndiotactic propene−butene copolymers confirm that it is possible to make out a precise regulation of the crystal modification of polymorphic polymer from the internal crystalline lattice via isomorphic crystallization.

## Conclusion

In this study, we revealed an example of regulating the crystalline modification of polymorphic polymer from the internal crystalline lattice. The modification of polymorphic polyester can be regulated from the internal crystalline lattice via the oriented isomorphic crystallization of random copolyester. As a typical example for this study, the random copolyester of butylene adipate (BA) and hexamethylene adipate (HA) units exhibits isodimorphic crystallization. The PBA type crystalline structure develops in the P(HA-*co*-BA)s with the HA unit content up to 34 mol %. Particularly, the PBA $\beta$-form crystal was highly favored in the PBA type crystal due to the cocrystallization of the HA and the BA units in the crystalline phase. The mechanism for the regulation of the crystal modification of PBA formed in P(HA-*co*-BA) copolyesters depends on that the HA units are selectively compatible with the PBA $\beta$-form crystal rather than the PBA α-form crystal. Therefore, the increase of the HA units in P(HA-*co*-BA) copolyester favors the formation of the PBA $\beta$-form crystal. As a conclusion, these results confirm the possibility of a precise regulation of crystalline modification of polymorphic polyester from the internal crystalline lattice via isomorphic crystallization.

## References and Notes


(1) Pan, P.; Inoue, Y. *Prog. Polym. Sci.* **2009**, *34*, 605–640.
(2) De Rosa, C.; Auriemma, F. *Prog. Polym. Sci.* **2006**, *31*, 145–237.
(3) Lotz, B.; Wittmann, J. C.; Lovinger, A. J. *Polymer* **1996**, *37*, 4979–4992.
(4) Bruckner, S.; Meille, S. V.; Petraccone, V.; Pirozzi, B. *Prog. Polym. Sci.* **1991**, *16*, 361–404.
(5) Corradini, P.; Guerra, G. *Adv. Polym. Sci.* **1992**, *100*, 183–217.
(6) Libster, D.; Aserin, A.; Garti, N. *Polym. Adv. Technol.* **2007**, *18*, 685–695.
(7) Grein, C.; Plummer, C. J. G.; Kausch, H. H.; Germain, Y.; Beguelin, Ph. *Polymer* **2002**, *43*, 3279–3293.
(8) Lovinger, A. J. *Science* **1983**, *220*, 1115–1121.
(9) Iwata, T.; Aoyagi, Y.; Tanaka, T.; Fujita, M.; Takeuchi, A.; Suzuki, Y.; Uesugi, K. *Macromolecules* **2006**, *39*, 5789–5795.
(10) Tanaka, T.; Yabe, T.; Teramachi, S.; Iwata, T. *Polym. Degrad. Stab.* **2007**, *92*, 1016–1024.
(11) Furuhashi, Y.; Iwata, T.; Kimura, Y.; Doi, Y. *Macromol. Biosci.* **2003**, *3*, 462–470.
(12) Zhu, B.; He, Y.; Nishida, H.; Yazawa, K.; Ishii, N.; Kasuya, K.; Inoue, Y. *Biomacromolecules* **2008**, *9*, 1221–1228.
(13) Zhu, B.; He, Y.; Asakawa, N.; Yoshie, N.; Nishida, H.; Inoue, Y. *Macromol. Rapid Commun.* **2005**, *26*, 581–585.
(14) Guerra, G.; Di Dino, G.; Centore, R.; Petraccone, V.; Obrzut, J.; Karasz, F. E.; Mac Knight, W. J. *Makromol. Chem.* **1989**, *190*, 2203–2210.
(15) Zhao, L.; Gan, Z. *Polym. Degrad. Stab.* **2006**, *91*, 2429–2436.
(16) Woo, E. M.; Sun, Y. S.; Yang, C. P. *Prog. Polym. Sci.* **2001**, *26*, 945–983.
(17) Miyazaki, T.; Takeda, Y.; Akasaka, M.; Sakai, M.; Hoshiko, A. *Macromolecules* **2008**, *41*, 2749–2753.
(18) Papageorgiou, G. Z.; Vassiliou, A. A.; Karavelidis, V. D.; Koumbis, A.; Bikiaris, D. N. *Macromolecules* **2008**, *41*, 1675–1684.
(19) Bluhm, T. L.; Hamer, G. K.; Marchessault, R. H.; Fyfe, C. A.; Veregin, R. P. *Macromolecules* **1986**, *19*, 2871–2876.
(20) Allegra, G.; Bassi, I. W. *Adv. Polym. Sci.* **1969**, *6*, 549–574.
(21) Mochizuki, M.; Mukai, K.; Yamada, K.; Ichise, N.; Murase, S.; Iwaya, Y. *Macromolecules* **1997**, *30*, 7403–7407.
(22) Papageorgiou, G. Z.; Bikiaris, D. N. *Biomacromolecules* **2007**, *8*, 2437–2449.
(23) Li, X.; Sun, J.; Huang, Y.; Geng, Y.; Wang, X.; Ma, Z.; Shao, C.; Zhang, X.; Yang, C.; Li, L. *Macromolecules* **2008**, *41*, 3162–3168.
(24) Liang, Z.; Pan, P.; Zhu, B.; Dong, T.; Hua, L.; Inoue, Y. *Macromolecules* **2010**, *43*, 2925–2932.
(25) Minke, R.; Blackwell, J. *J. Macromol. Sci., Phys.* **1979**, *B16*, 407–417.
(26) Minke, R.; Blackwell, J. *J. Macromol. Sci., Phys.* **1980**, *B18*, 233–255.
(27) Pouget, E.; Almontassir, A.; Casas, M., T.; Puiggalí, J. *Macromolecules* **2003**, *36*, 698–705.
(28) Gestí, S.; Almontassir, A.; Casas, M. T.; Puiggalí, J. *Biomacromolecules* **2006**, *7*, 799–808.
(29) Kai, W.; Zhu, B.; He, Y.; Inoue, Y. *J. Polym. Sci., Part B: Polym. Phys.* **2005**, *43*, 2340–2351.
(30) Dong, T.; Kai, W.; Inoue, Y. *Macromolecules* **2007**, *40*, 8285–8290.
(31) Sun, Y.; Li, H.; Huang, Y.; Chen, E.; Zhao, L.; Gan, Z.; Yan, S. *Macromolecules* **2005**, *38*, 2739–2743.

(32) Sun, Y.; Li, H.; Huang, Y.; Chen, E.; Gan, Z.; Yan, S. *Polymer* **2006**, *47*, 2455–2459.
(33) Gan, Z.; Kuwabara, K.; Abe, H.; Iwata, T.; Doi, Y. *Biomacromolecules* **2004**, *5*, 371–378.
(34) Gan, Z.; Abe, H.; Doi, Y. *Macromol. Chem. Phys.* **2002**, *203*, 2369–2374.
(35) Cranston, E.; Kawada, J.; Raymond, S.; Morin, F. G.; Marchessault, R. H. *Biomacromolecules* **2003**, *4*, 995–999.
(36) De Rosa, C.; Auriemma, F.; de Ballesteros, O. R.; Resconi, L.; Camurati, I. *Macromolecules* **2007**, *40*, 6600–6616.
(37) De Rosa, C.; Auriemma, F.; de Ballesteros, O. R.; De Luca, D.; Resconi, L. *Macromolecules* **2008**, *41*, 2172–2177.
(38) De Rosa, C.; Talarico, G.; Caporaso, L.; Auriemma, F.; Galimberti, M.; Fusco, O. *Macromolecules* **1998**, *31*, 9109–9115.
(39) De Rosa, C.; Auriemma, F.; Orlando, I.; Talarico, G.; Caporaso, L. *Macromolecules* **2001**, *34*, 1663–1672.
(40) De Rosa, C.; Auriemma, F.; Caliano, L.; Talarico, G.; Corradi, M. *Macromolecules* **2008**, *41*, 5301–5306.
(41) De Rosa, C.; Auriemma, F.; Corradi, M.; Caliano, L.; Talarico, G. *Macromolecules* **2008**, *41*, 8712–8720.